LA-UR- 10-00425

Approved for public release;
distribution is unlimited.

Title:	The solubility of hydrogen and deuterium in alloyed, unalloyed and impure plutonium metal
Author(s):	Richmond S Bridgewater J Ward J Allen T
Intended for:	Proceedings of JOWOG 22-8

Los Alamos
NATIONAL LABORATORY
EST. 1943

Form 836 (7/06)

The solubility of hydrogen and deuterium in alloyed, unalloyed and impure plutonium metal

Scott Richmond, Jon Bridgewater, John Ward, Thomas Allen

Los Alamos National Laboratory, Los Alamos, NM, USA

Abstract

Hydrogen is exothermically absorbed in many transition metals, all rare earths and the actinides. The hydrogen gas adsorbs, dissociates and diffuses into these metals as atomic hydrogen [1,2]. Absorbed hydrogen is generally detrimental to Pu, altering its properties and greatly enhancing corrosion [3]. Measuring the heat of solution of hydrogen in Pu and its alloys provides significant insight into the thermodynamics driving these changes. Hydrogen is present in all Pu metal unless great care is taken to avoid it. Heats of solution and formation are provided along with evidence for spinodal decomposition.

1. Introduction

Hydrogen absorbs into a metal, *M*, by a process of adsorption, dissociation and dissolution into the metal [5]. At equilibrium the chemical potential of the gas, μ^g, is equal to the chemical potential of hydrogen in the metal, $\mu(H/M)$. The solution equilibrium condition is,

$$M + \frac{x}{2} H_2 \xleftrightarrow{K_S} MH_x \,, \tag{1}$$

$$\tfrac{1}{2}\mu^g = \mu(H/M). \tag{2}$$

In equation (1) K_S is the equilibrium constant, also known as the Sieverts' constant, is given by:

$$K_S = \frac{H}{M} \cdot \left(\frac{p}{p_0}\right)^{-\frac{1}{2}} \quad \text{or, less formally,} \quad K_S = \frac{H}{M} \cdot \sqrt{p} \tag{3}$$

Equation (3), is generally attributed to Adolf Sieverts (1874-1947) and known as Sieverts' law [5,6,7] which shows that at equilibrium *H/M* varies proportionally with the square root of the pressure, *p*, indicating that atomic hydrogen, *H*, rather than H_2, is in solution in the metal. Equation (3) is generally valid for a dilute solution, less than a few percent *H/M*, and low pressures (<100 ATM) [4]. The value of p_0 is customarily one atmosphere (1 ATM) for historical consistency. The Sieverts' constant varies in an Arrhenius fashion, so a plot of $\ln(K_S)$ versus $1/T$ has a line whose slope is the heat of solution, ΔH_S, of hydrogen in the metal, divided by the gas constant. Consequently,

$$K_S = K_0 \cdot e^{-\frac{\Delta H_S}{RT}} \cdot e^{\frac{\Delta S^{nc}}{R}} \tag{4}$$

describes the solubility of hydrogen in a metal as a function of the heat and entropy (non-configurational) of solution, ΔH_S and ΔS^{nc}, and absolute temperature, *T*. *R* is the gas

constant. If K_0 is known and the $\ln(K_S/K_0)$ is plotted versus $1/T$ then the intercept of the line, where $1/T$ approaches 0 ($T=\infty$), is the non-configurational entropy of solution, ΔS^{nc}, divided by the gas constant, R.

If the heats of solution, ΔH_S, and non-configurational entropy of solution, ΔS^{nc}, are known for each allotropic solid phase and the liquid phase, then the solvus line of the Pu-H phase diagram can be established for all temperatures and compositions where the free energy of solution, ΔG_S, is equal to the free energy of formation of the dihydride (PuH_2), ΔG_F. In other words, at the solvus line:

$$\Delta G_S = \Delta G_F = \Delta H_S - T \cdot \Delta S^{nc} = \Delta H_F - T \cdot \Delta S_F \qquad (5)$$

The solvus line is the point of maximum hydrogen in solution in equilibrium with the dihydride. At this point, at a given temperature, the addition of any hydrogen to the metal results in precipitation of the dihydride because it is a saturated solution. It is plutonium metal in this condition that Haschke et. al. [3] have shown is extremely susceptible to corrosion. This whitepaper details the nature of hydrogen incorporation from hydrogen free to saturated solution for alloyed and unalloyed Pu.

2. Understanding and using Pressure-Composition-Temperature isotherms.

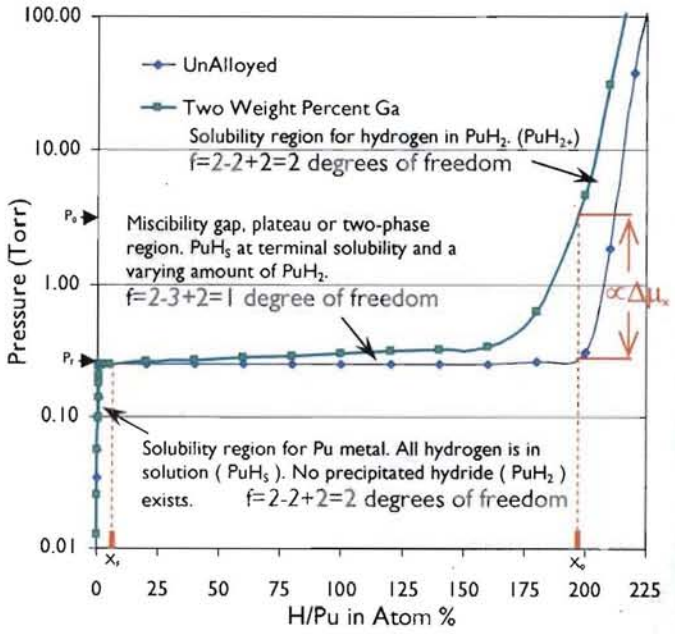

Figure 1. Pu-H Pressure-Composition-Temperature isotherms at 475°C (Allen [2]).

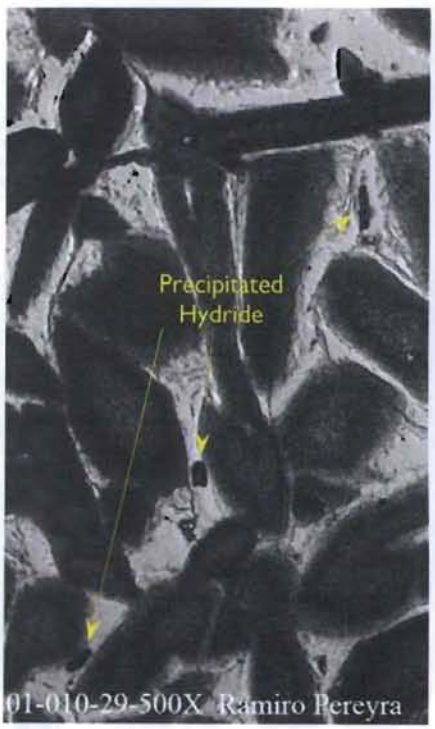

Figure 2. Hydride in regions with low gallium (light grey).

By creating Pressure-Composition-Temperature (PCT) isotherms like those shown in figure 1 for unalloyed and alloyed Pu we can learn where and when hydride

will precipitate. The isotherms in figure 1 have three regions. In the far left hand region, hydrogen is completely soluble in the metal, in the middle a region, the metal is saturated with and precipitates as PuH_2. In the far right hand region, all PuH_2 has precipitated and hydrogen dissolves in PuH_2 (PuH_{2+x}). Applying the Gibbs' phase rule to figure 1 reveals important characteristics of these isotherms. The Gibbs' phase rule states that the number of degrees of freedom, f, of a system is equal to the number of components, C, minus the number of thermodynamic phases, P, plus 2.

$$f = C - P + 2 \qquad (6)$$

Both curves in figure 1 start out on the left (H/Pu=0) and as hydrogen is added to the system H/Pu increases and so does the pressure. In the solubility region there are 2 components, the gas and the metal, and two phases, gas and solid. Consequently in the solution region there are two degrees of freedom, f=2-2+2=2.

When the metal becomes saturated with hydrogen a new phase appears, PuH_2, and solubility has reached a terminal value. From this point on, until a stoichiometric concentration of hydrogen for PuH_2 is created in the metal, the addition of hydrogen to the metal will result in precipitation of the hydride phase. This is the two phase region of the metal[1] where, f=2-3+2=1; only one degree of freedom exists. Because only one degree of freedom exists for the hydrogen saturated unalloyed Pu, the addition of hydrogen occurs without a pressure increase until all the Pu is converted to PuH_2. The PCT curve for unalloyed Pu is a nearly ideal case of the phase rule. However the two weight percent Ga alloyed Pu retains a degree of freedom in the plateau region that is much smaller than in the solubility region. The slope in the Ga alloyed Pu plateau makes it evident that not all of the hydrogen added beyond saturation will incorporate as PuH_2. Some of the hydrogen continues to go into solution in a new *component* that competes with PuH_2.

Finally, when the Pu has been fully converted to PuH_2, hydrogen continues to dissolve into the PuH_2. This the last portion of the curves in figure 1 (right hand side). No more phase change is occurring as hydrogen is being added, f=2-2+2, so there are two degrees of freedom again. The additional component that "grew in" during hydride formation in the two weigh percent Ga alloy remains present in the PuH_{2+x} solution region but stops growing in.

An important fact to note about the two curves is that their equilibrium pressures are not equal. Because the alloy has a higher equilibrium pressure for a given composition than the unalloyed Pu, the unalloyed Pu will be the thermodynamically favored site for hydride formation. This case is illustrated in figure 2. Figure 2 is a metallograph of unhomogenized ("cored") Pu-Ga alloy containing hydride in the Ga lean regions (light grey) as predicted by the PCT data. The dark grey regions in figure 2 are Ga rich and contain little or no precipitated hydride.

Using figure 1 as an example it can be shown why hydride must occur in the Ga lean or unalloyed regions of the Pu in figure 2. Assume that we have two separate samples containing equal amounts of Pu, both at 475°C, and one being unalloyed Pu while the other is 2 wt.% Ga. If we also assume that the 2 wt.% Ga sample contains an initial concentration of H/Pu equal to x_0 (see figure 1)and the unalloyed sample contains no hydrogen at all, then, by virtue of equations (1,2,3), we would expect that the

[1] The metal is two phase, Pu and PuH_2, but the system has 3 phases, gas, metal and precipitated hydride.

hydrogen gas pressure in equilibrium with the 2 wt.% Pu to be about 3 Torr (P_0 on figure 1) while unalloyed Pu containing no *H* would be at a hard vacuum (below the scale of figure 1). So if we then placed the gas phase of the 2 wt.% Ga Pu sample in communication with the unalloyed Pu sample, the hydrogen gas will flow into the unalloyed sample until the gas phase pressures equalize. When the pressures are equal (P_F in figure 1) then concentration, as *H/Pu* in the 2 wt.% Ga Pu sample will be x_F and the concentration in the unalloyed Pu sample will be x_0-x_F. Even if the two samples were not separate, but rather were a heterogeneous composition similar to that of figure 2 the concentration would similarly adjust because a difference in chemical potential, $\Delta\mu$, exits until the concentration of hydrogen in the two alloy compositions adjusts to balance the chemical potential. The difference in chemical potential at a given temperature is given by:

$$\Delta\mu = R \cdot T \cdot \ln\left(\frac{p_f}{p_0}\right). \tag{7}$$

In the case where a chemical potential exists within a heterogeneous composition (across a distance x) as a result of hydrogen in the metal, a force, F, will arise:

$$F = \frac{\partial\mu}{\partial x}. \tag{8}$$

Consequently, hydrogen in solution (mobile H atoms) will move as a result of (8) until $\Delta\mu$=0. As we can see in figure 1 and 2, when $\Delta\mu$=0 in a heterogeneous Pu alloy composition, the concentration of hydrogen will vary depending on the local alloy composition.

By measuring PCT isotherms in Pu and pure alloys of Pu we can establish where in the metal hydrogen will concentrate, identify phase boundaries and provide equations to relate measured hydrogen concentrations (H/Pu) to hydrogen pressures as an aid to removing it from the metal and preventing corrosion.

3. Pressure-Composition-Temperature measurement.

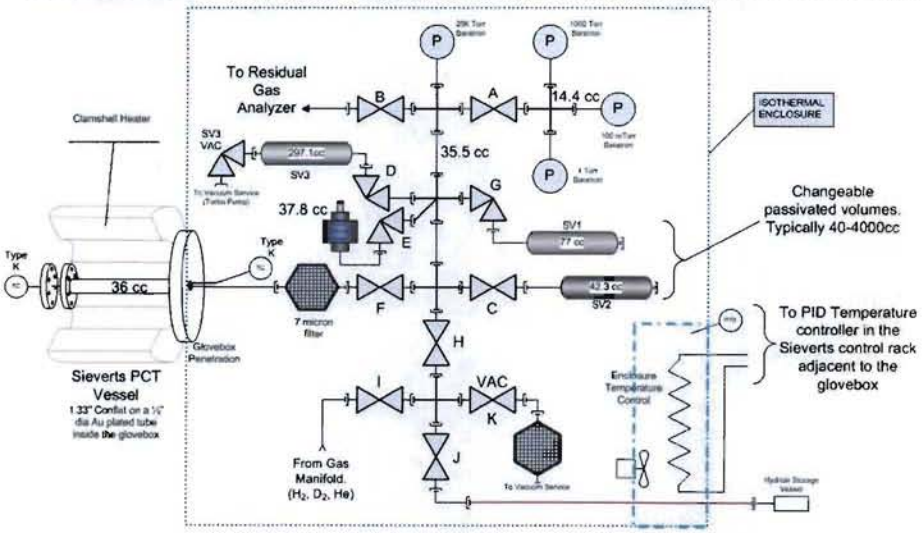

Figure 3. Sieverts' apparatus used for Pu-H Pressure-Composition-Temperature isotherms.

PCT measurements are made using a Sieverts type apparatus [7]. In the Sieverts apparatus a vessel which contains the sample (~1 to 2 g) was held at constant temperature and measured quantities of gas were equilibrated either to or from the sample via a second vessel of known volume. The equilibrium pressure of the gas during each addition or removal of gas was recorded. Between equilibrations the sample in the vessel was isolated from the equilibrium vessel with a valve and the equilibrium vessel was either evacuated in the case of desorption or filled to a desired pressure in the case of absorption. Based on the ideal gas law, the equilibrium vessel pressure, temperature and volume were used to determine the amount of hydrogen in the sample at each point. The data obtained in this way is placed into a pressure-composition-temperature plot or PCT. A series of PCT isotherms were produced in this fashion for pure Pu and Pu-2 at.%-Ga using pure hydrogen and deuterium. The accuracy of the temperature measurement is ±2°C, and pressure ±0.1% of full scale. A 1 and 1000 Torr and 100 mTorr capacitance manometer were used. The accuracy of the volumes used is ±4%. Sample masses are a measured to within 5 mg. Measurements above melt were conducted by Allen in an apparatus documented previously [2].

4. Pressure-Composition-Temperature isotherm data.

P-C-T data (P vs. H/Pu) are shown in figures 4-9.

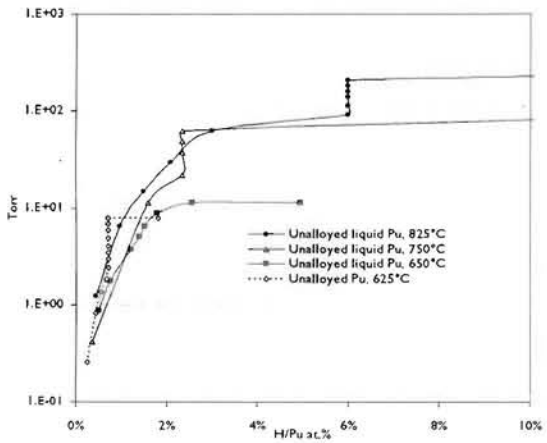

Figure 4. H_2 absorption isotherms for unalloyed liquid Pu by Allen [2].

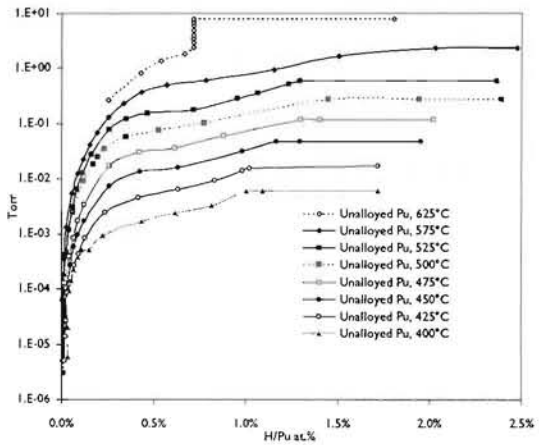

Figure 5. H_2 PCT absorption isotherms for solid unalloyed Pu.

The H_2 absorption PCT isotherms for unalloyed Pu are shown in figures 4 and 5. PuH_2 is evidently a solid with a melting point above 825°C because the pressure increases appreciably at the terminal solubility of H in liquid Pu with no compositional change (H/Pu is constant), due to the heat of fusion of PuH_2. The same feature is evident at 625°C, 15°C below the melting point of Pu, indicating depression of the Pu melting point. The 625°C sample did not appear to be melted but did stick to its sample holder, so that sample appears to have experienced partial melting. The heat of fusion of PuH_2 is estimated from this data to be 8679 J/mol. (~0.1eV). The same 625°C isotherm is included on both the liquid and solid plots. The solid unalloyed Pu isotherms all display

an inflection at about 0.6-0.7 at.% H/Pu. This inflection was first noted by Allen [2] in 1991 but could not be explained. The observed inflection can be explained as spinodal decomposition since the measured pressure is in equilibrium with the hydrogen in the metal (2) and since spinodal decomposition requires

$$\frac{\partial^2 \mu}{\partial x^2} < 0, \tag{9}$$

where x=H/Pu, then the inflection is the consequence of (2) and (9) on the measured pressure. The effect is described in detail by Fukia in sections 2.2 and 2.3 of [5] and is the result of attractive H-H interactions. The general principles of spinodal decomposition are detailed by Hillert [8] and Cahn [9] as compositional variations that result in a reduced free energy state (i.e. they are stable). These variations are stable and occur uniformly throughout the material unlike nucleation which only occurs only at specific sites.

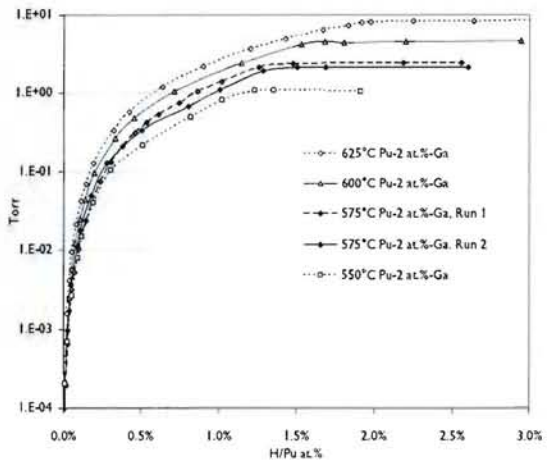

Figure 6. H_2 PCT absorption isotherms for solid Pu-2 at.%-Ga from 550-625°C.

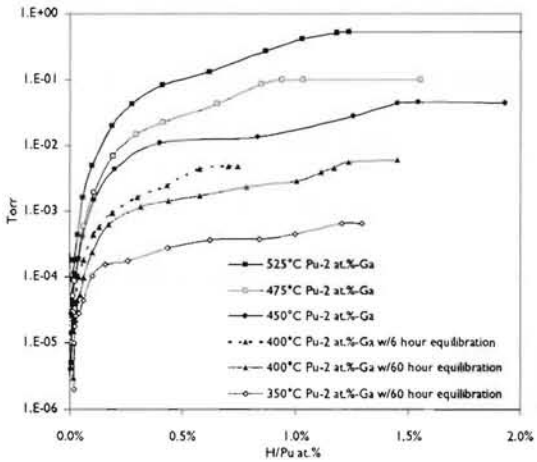

Figure 7. H_2 PCT absorption isotherms for solid Pu-2 at.%-Ga from 350-525°C.

The H_2 absorption PCT isotherms for Pu-2 at.%-Ga in the temperature range 350-625°C are shown in figures 6 and 7 .The inflection observed in unalloyed isotherms is also significant below 550°C in Pu-2 at.%-Ga H_2 isotherms (figure 7). Figure seven includes two curves run at 400°C, both run on the same coupon. The first was run quickly, allowing only the hydrogen gas to equilibrate with the metal, but during this run a true thermodynamic equilibrium was not achieved as evidenced by a very slow drift in the pressure. Mulford and Sturdy also noted that equilibration times at temperatures below ~450°C were very long [2]. A second curve was run at 400°C allowing full equilibration and the second curve is also shown in figure 7.

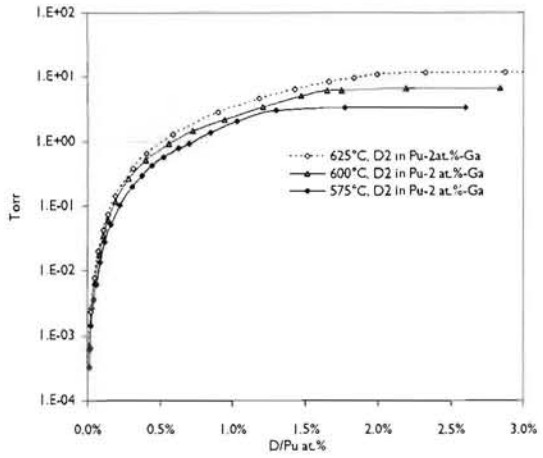

Figure 8. D_2 PCT absorption isotherms for solid Pu-2 at.%-Ga from 575-625°C.

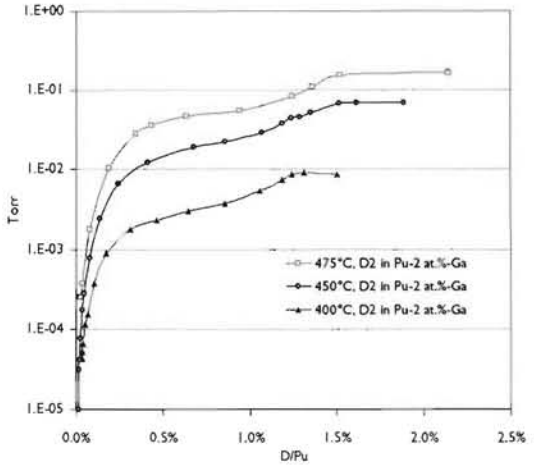

Figure 9. D_2 PCT absorption isotherms for solid Pu-2 at.%-Ga from 400-475°C.

The D_2 absorption PCT isotherms for Pu-2 at.%-Ga in the temperature range 400-625°C are shown in figures 8 and 9.The D_2 absorption isotherms exhibited behavior similar to the H_2 isotherms for Pu-2at.%-Ga as expected. Deuterium isotherm pressures for a given composition were typically higher than protium isotherm pressures at the same composition by a factor of $\sqrt{2}$.

5. Interpretation of the isotherm data.

The data shown in figures 4-9 is plotted as $p^{1/2}$ versus composition and a Sieverts' constant is determined. Figures 10 and 11 show the Sieverts' plots for hydrogen in Pu-2 at.%-Ga.

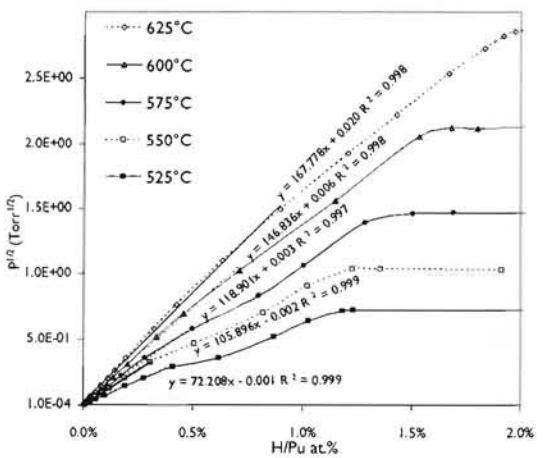

Figure 10. Sieverts' Plot for H_2 in Pu-2 at.%-Ga from 575-625°C showing linear fit.

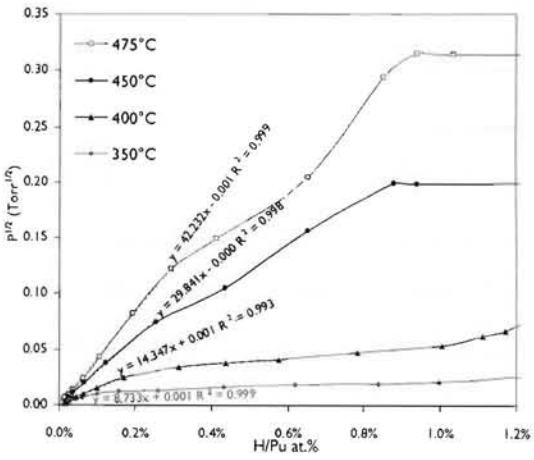

Figure 11. Sieverts' plot for H_2 in Pu-2 at.%-Ga from 350-475°C showing linear fit.

In the linear region of each data set, a fit is obtained. The fit is only applied in the dilute solution region where linear square root behavior conforms to Sieverts' Law (3). The linear fit is the equation of a line where $y=mx+b$ and b is very nearly zero in each case. So that the Sieverts' constant is taken from these plots as $K_S=1/m$ (as in (3) but neglecting p_0). The Sieverts' constants were similarly obtained for H_2 in unalloyed Pu and for D_2 in Pu-2 at.%-Ga. The $\ln(K_S)$ vs. $1/T$ of the data obtained is shown in figure 12.

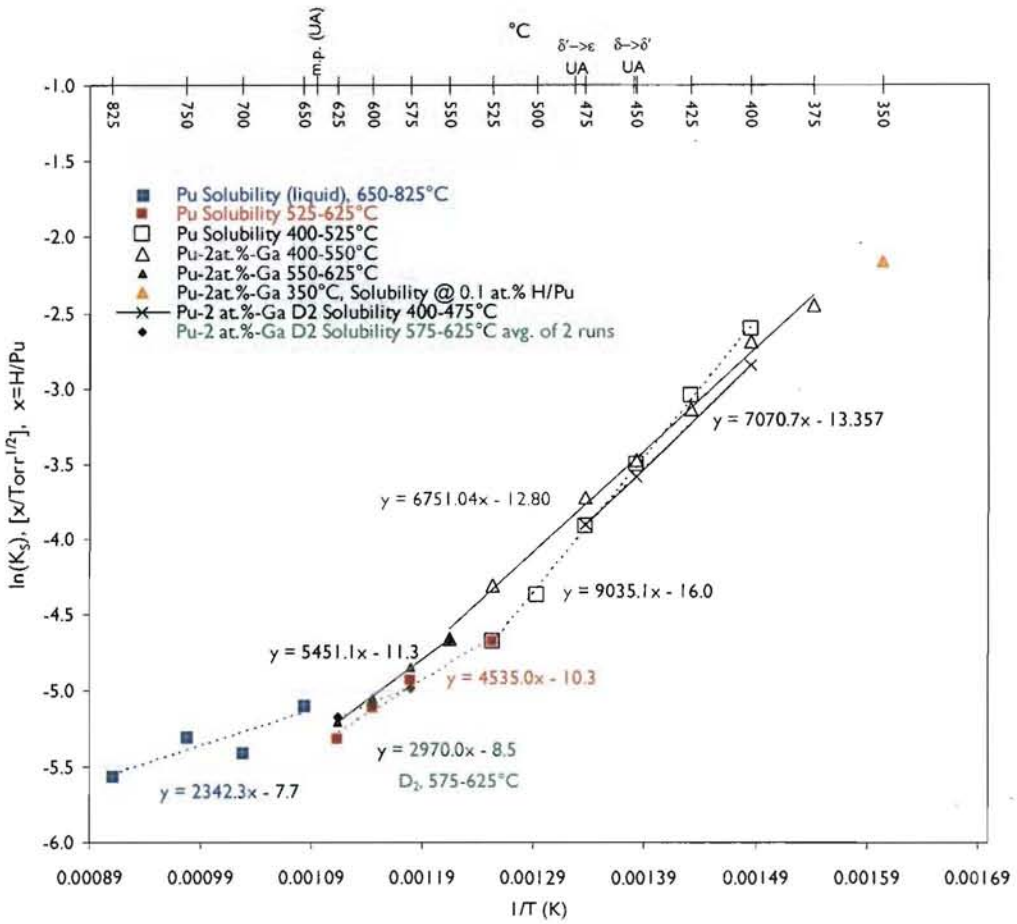

Figure 12. Arrhenius plot of the natural log of the Sieverts' constants, K_S, for H_2 and D_2 in Pu-2 at.%-Ga and H_2 in unalloyed (UA) Pu. The unalloyed Pu melting point (m.p.), δ→δ′ and δ′→ε transition temperatures are noted on the upper scale. The Pu-2 at.%-Ga δ→(δ + ε) occurs at ~476°C.

Each set of data has a best fit line of the form $y=mx+b$. Multiplying the slope (m) of a given fit by the gas constant (R=8.314 J·mol^{-1}·K^{-1}) gives the heat of solution:

$$\Delta H_S = -R \cdot \frac{\partial \ln(K_S)}{\partial \frac{1}{T}}. \qquad (10)$$

The energies obtained from each fit shown in figure 12 are listed in Table 1. Wipf [4] has shown that enthalpies and entropies of solution can also be determined from the pressure isotherm data at constant composition and very dilute solution ($x<<r$), where:

$$\Delta H_S = \tfrac{1}{2} \cdot R \cdot \left. \frac{\partial \ln(p/p_0)}{\partial \frac{1}{T}} \right|_{X=\text{const.}}, \qquad (11)$$

$$\Delta S^{nc} = R \cdot \ln(\tfrac{x}{r}) - \tfrac{1}{2} \cdot R \cdot T \cdot \left. \frac{\partial \ln(p/p_0)}{\partial T} \right|_{X=\text{const.}}. \qquad (12)$$

The value of r in equation (12) is the number of interstitial sites per Pu atom and x is the composition (H/Pu). The entropies of solution in Table 1 were determined using (12) on the data of figures 4-9. Since the value of r is unknown, a plot of $\frac{1}{2} \cdot R \cdot T \cdot \ln(p/p0)$ versus T for a fixed value of x was used to get a line whose slope is ΔS^{nc} for a fixed concentration (x) over the temperature ranges associated with each plot in figure 12. The non-configurational entropies determined in this manner for the concentrations associated with the solubility values in figure 12 are also shown in table 1.

Table 1. Heats of solution and non-configurational entropies of solution based on figure 12.

	ΔH_S (J·mol^{-1})	ΔH_S (eV)	ΔS^{nc} (J·mol^{-1} K^{-1})	ΔS^{nc} k_B^{-1} [a]
liquid Pu (>639.5°C)	-19473	-0.20	05.5	0.7
Pu, 525-625°C @ H/Pu=0.25 at.%	-37704	-0.39	07.5	0.9
Pu, 400-525°C @ H/Pu=0.2 at. %	-75118	-0.78	54.0	6.5
H in Pu-2 at.%-Ga 550-625°C	-45320	-0.47	21.0	2.5
H in Pu-2 at.%-Ga 400-550°C	-56167	-0.58	49.0	5.9
D in Pu-2 at %-Ga 575-625°C	-24693	-0.26	-	-
D in Pu-2 at %-Ga 400-475°C	-58786	-0.61	-	-

[a] k_B is the Boltzmann constant in eV·K^{-1} (8.617e-5 eV K^{-1})

The data in figure 12 shows a clear change in solubility above the 640°C melting point. The best fit line for solubility in the liquid region, if projected to the unalloyed solid solution, intercepts at 533°C. The free energy of solution is sufficient to permit partial melting below 640°C and that is supported by the observations made in figures 4 and 5 where a pressure transition characteristic of a phase change (heat of fusion) occurs on the 625°C unalloyed isotherm. Solubility measurements between 533°C and 640°C have values intermediate to those above or below, further indicating a mixed phase of liquid+ ε.

Notably absent in figure 12 are inflections in the solubility at the δ⟶ε and δ⟶δ'⟶ε transition temperature regions for alloyed (500-525°C) and unalloyed (451-476°C) Pu respectively. An inflection should have been present in these temperature ranges because δ-Pu has a face centered cubic (fcc) lattice structure with one octahedral and two tetrahedral interstitial sites per Pu atom while ε-Pu has a body centered cubic (bcc) lattice structure with three octahedral and six tetrahedral interstitial sites per Pu atom. Consequently the bcc structure is more soluble to hydrogen than the fcc structure. X-ray data is needed to determine why a change in solubility was not observed in these temperature ranges, but presently this capability is unavailable under these conditions for Pu.

Departure from ideal solution behavior.

The data obtained and summarized by figure 12 are only valid at dilute solution conditions. In figure 11 it can be seen that the linear portion of the $P^{1/2}$ vs. H/Pu plot is

limited to very low concentrations, for example < 0.2 at.% H/Pu for the 400°C data. Beyond the Sievert's region ($P^{1/2}$ α H/M) the metal becomes increasingly soluble to hydrogen with increasing hydrogen content. This tendency is attributed to attractive H-H interactions [5] and is observed in many metals. However, this tendency increases much more rapidly in Pu than in other metals. The region of extended solubility has varying enthalpy and entropy, which are greater than the Sievert's region but less than the enthalpy and entropy for formation of PuH_2. The region of "extended solubility" is the spinodal decomposition described earlier. The slow onset of spinodal decomposition is most significant below ~450°C where it affects the majority of the solution region. Equilibration times in this region are about 100 times slower than in the Sieverts region or at the plateau, typically 10-15 hours vs. 20 minutes. Very slow equilibration times below 450°C were also noted by Mulford and Sturdy [2] in their Pu hydriding studies.

Heats of formation.

Heats of formation are obtained from the data of figures 4-9 and are compared to other researcher's results in figure 13.

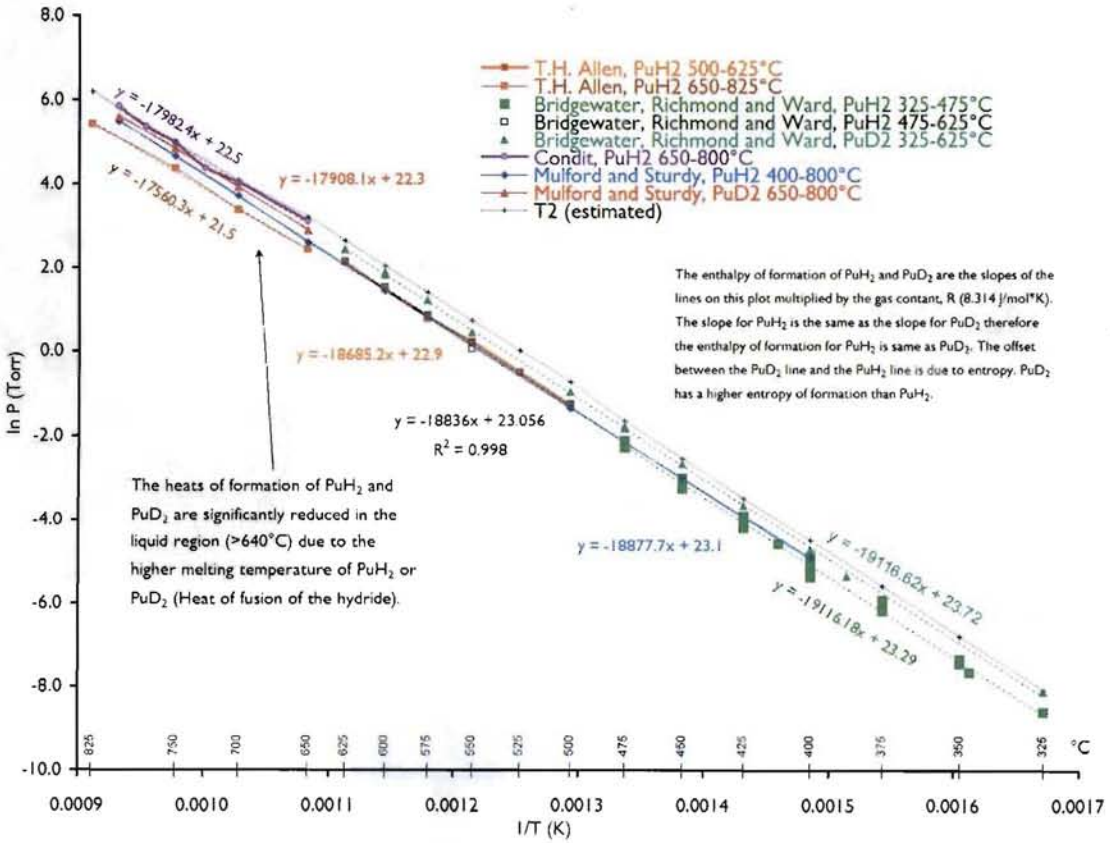

Figure 13. Arrhenius plot of the natural log of the hydrogen pressure, *P*, for H_2 and D_2 in unalloyed Pu.

Table 2. Heats and entropies of formation based on figure 13.

	ΔH_f (J·mol^{-1})	ΔH_f (eV)	ΔS_f (J·mol^{-1}·K^{-1})	$\Delta S_f \cdot k_B^{-1}$ [a]
PuH_2 (>639.5 C, liquid Pu) Allen [2]	-145996	-1.51	123.6	14.9
PuH_2 (>639.5 C, liquid Pu) Condit [2]	-149506	-1.55	131.9	15.9
PuD_2 (>639.5 C, liquid Pu) Mulford and Sturdy [2]	-148887	-1.54	130.3	15.7
PuH_2 (400-800 C) Mulford and Sturdy [2]	-156949	-1.63	136.9	16.5
PuD_2 (325-625 C) this work	-158935	-1.65	142.1	17.1
PuH_2 (475-625 C) this work	-156602	-1.62	136.5	16.4
PuH_2 (325-475 C) this work	-158932	-1.65	138.5	16.7

[a] k_B is the Boltzmann constant in eV·K^{-1} (8.617e-5 eV·K^{-1})

6. The solubility of hydrogen in impure Pu metal.

Many hydrogen solubility measurements of Pu samples were conducted, but two alloy compositions produced unusual results, one with Fe at a level just above the solid solution limit and another with a very low Ga content (500 wppm). The isotherms are shown in Figures 14 and 15.

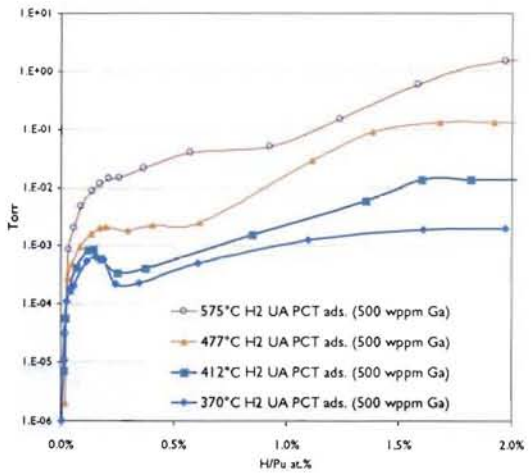

Figure 14. H_2 PCT absorption isotherms for low Ga Pu.

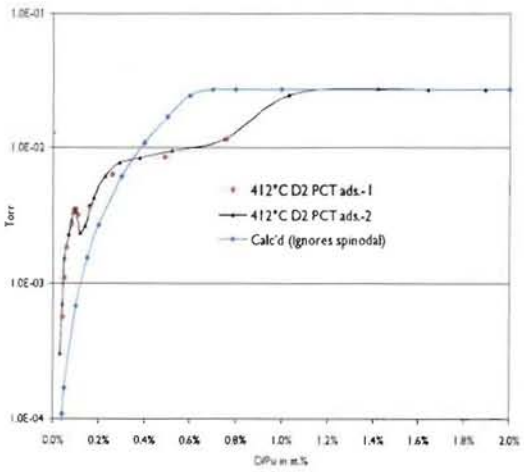

Figure 15. D_2 PCT absorption isotherms for Pu-2 at.%-Ga containing Fe impurities.

The data in Figure 14 shows that at 370-412°C as hydrogen was dissolved into the δ-phase Pu the pressure at first increased as expected, but at about 0.2 at.% H/Pu, adding H resulted in a decrease in the equilibrium pressure until about 0.4 at.% H/Pu. This means the free energy was at first decreasing but subsequently increased and finally decreased again until the two phase region (plateau) was reached. The pressure reversal effect diminished as temperature was increased. Figure 11 is a plot of two equilibrium isotherms for Pu-2 at.%-Ga with Fe impurities just above the solubility limit for Fe in Pu (~0.15 at.%). The data is qualitatively similar to that in Figure 14; however the points in Figure 15 only required about 15 minutes to equilibrate vs. 15 hours for the points in Figure 14. Data was taken for Pu-2 at.%-Ga with Fe impurities from 400-625°C and it was found that equilibration times were always very short in the iron bearing samples,

but that the isotherms were otherwise similar to Pu-2at.%-Ga without Fe. Only the 412°C Pu sample with Fe impurities displayed the pressure/free energy inflection. 412°C is, perhaps coincidentally, the temperature at which the Pu_6Fe intermetallic compound has a solid to liquid transition. Data for the Fe impure material was taken a second time to verify the presence of the inflection and measure it more precisely. A calculated curve for D in Fe-free material is also shown in figure 15. It is not known why the pressure inflections occurred, however the fact that they did occur means the chemical potential, $\mu(H/M)$, of solution has been lowered. In Figures 14 and 15, the 412°C isotherms can be bisected at single pressure and consequently a single $\mu(H/M)$ such that $\mu(x_1) = \mu(x_2) = \mu(x_3)$ .This is, again, characteristic of spinodal decomposition but more extreme; unfortunately x-ray data for Pu samples under these conditions is not presently available to confirm this definitively.

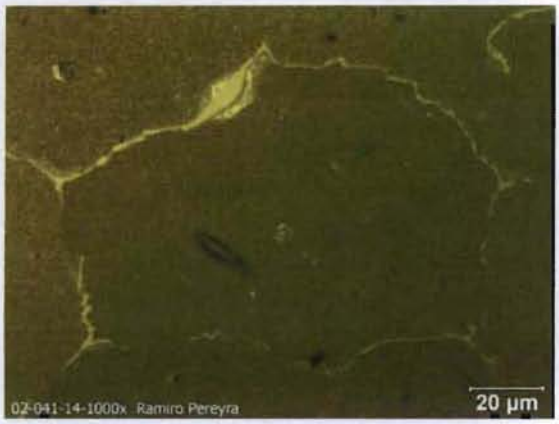

Figure 16. The lightly colored regions surrounding each grain are Pu_6Fe. The tan colored regions are δ-Pu and the light tan are α'-Pu.

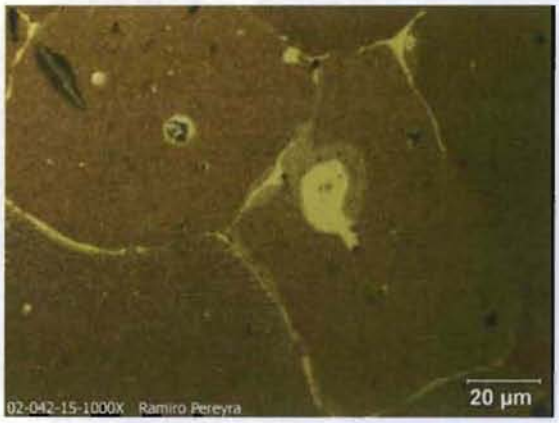

Figure 17. The dark regions surrounding many of the Pu_6Fe inclusions are hydride.

Metallography for Fe bearing samples, shown in figures 16 and 17, shows hydride strongly favors material immediately adjacent to Pu_6Fe inclusions. Figures 16 and 17 together with figure 15 indicate that the presence of an iron impurity allows hydrogen to enter a lower energy state than Fe free material. If the metallographer's assessment, that the lightly colored regions of figures 16 and 17 are α'-Pu, is correct, then that is consistent with the appearance of hydride in the same regions, because the free energy of solution is greater in lower Ga regions (according to our measurements, see figure 12). Quantitative measurements of the Ga concentration in these regions need to be performed to confirm this.

7. The plutonium-hydrogen solvus line.

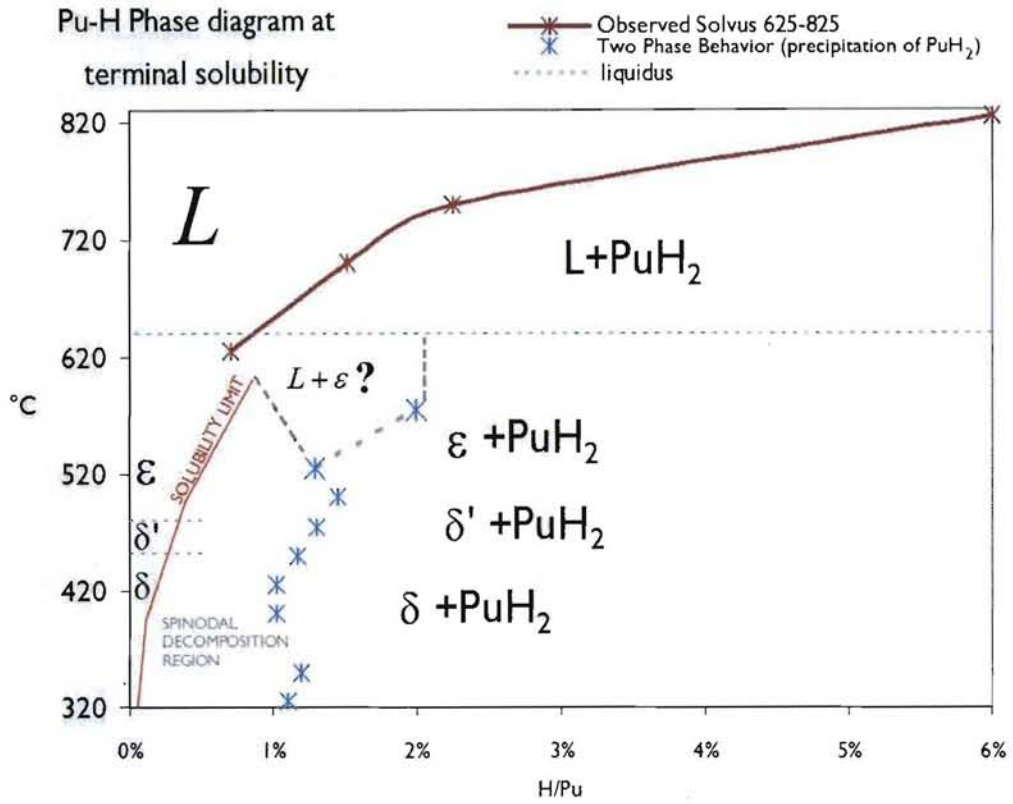

Figure 18. The solvus line and terminal solubility * of hydrogen in plutonium.

In order to eliminate PuH_2 precipitate in the metal, the hydrogen concentration must be reduced below the terminal solubility. The terminal solubility for Pu-H, the point at which any further addition of hydrogen results in the precipitation of PuH_2, is shown by the blue asterisks *. The true limit of solubility is shown by the red and dark red lines. The region between the red "solubility limit" and the blue asterisks is where attractive interactions between H atoms occur. This region is determined from the data like that in figures 10 and 11 but for unalloyed Pu. In figures 10 and 11 when the square root behavior ends, the conformance to Sieverts' Law (3) ends. Similarly, when the pressure no longer changes as H/Pu increases, then PuH_2 is precipitating. However there is a significant region in between these two (~1% H/Pu wide) where something else is happening. This region is the spinodal decomposition. In the spinodal decomposition region, attractive H-H interactions reduce the chemical potential and cause clustering of the hydrogen into spinodes [5]. The region just below melt but between the red solubility and blue asterisks (terminal solubility) is a region which appears to be a mixed phase of liquid+epsilon. The data in figure 12 indicates melt depression of a fraction of the solid

Pu in some (unknown) proportion to hydrogen (H/Pu). The indication of depressed melt is inferred from the intersection of the projection to lower temperature of the line fitted to the liquid solubility to the inflection in the solid solubilities at approximately 525°C and from the tendency of the higher entropy systems (unalloyed Pu-H, alloyed Pu-D) to inflect more severely in the direction of aligning with the liquid solubility. Additionally, only samples held above ~530°C tended to stick to their crucibles when the sample was unmelted. Partial melting with hydrogen in solution is thermodynamically favored, but we had no means to make a direct observation of this.

In order to reduce hydrogen (by means of a vacuum) below terminal solubility or the solubility limit, equations describing the hydrogen partial pressure for a given composition and temperature are useful. Equations, determined by the curve fits shown in figures 12 and 13, are given in table 3 and 4. Equations for the spinodal region are not provided (*tbd*).

Table 3. Equations for determining plateau hydrogen pressure for a given temperature.*

Temperature Range	H_2 Plateau P (Torr)	D_2 Plateau P (Torr)	T_2 Plateau P (Torr)
>639.5°C, liquid Pu	$P = e^{-17908*\frac{1}{T}+21.95}$	$P = e^{-17908.1*\frac{1}{T}+22.3}$	$P = e^{-17908.1*\frac{1}{T}+22.5}$
475°C to 639.5°C	$P = e^{-18836*\frac{1}{T}+23.056}$	$P = e^{-19116.2*\frac{1}{T}+23.72}$	$P = e^{-18836*\frac{1}{T}+23.61}$
<475°C	$P = e^{-19116.2*\frac{1}{T}+23.29}$	$P = e^{-19116.2*\frac{1}{T}+23.72}$	$P = e^{-19116.2*\frac{1}{T}+23.88}$

** T in Kelvin, T_2 plateau pressure is estimated (shaded expressions) based on the expected difference in entropy inferred from H and D entropies. A unity pre-exponential constant for dimensioning the expression to units of pressure is assumed (omitted for clarity).*

Table 4. Equations for determining the Sieverts' constant for a given temperature.*

Temperature Range	H_2 Solubility (H/Pu per$Torr^{½}$)	D_2 Solubility (D/Pu per$Torr^{½}$)	T_2 Solubility (T/Pu per$Torr^{½}$)
>639.5°C, unalloyed	$K_{S_H} = e^{2342.3*\frac{1}{T}-7.7}$	$K_{S_D} = e^{2342.3*\frac{1}{T}-8.05}$	$K_{S_T} = e^{2342.3*\frac{1}{T}-8.25}$
Unalloyed Pu, 525°C to 639.5°C	$K_{S_H} = e^{4535*\frac{1}{T}-10.3}$	$K_{S_D} = e^{4535*\frac{1}{T}-10.65}$	$K_{S_T} = e^{4535*\frac{1}{T}-10.85}$
Unalloyed Pu, 400°C to 525°C	$K_{S_H} = e^{9035*\frac{1}{T}-16.0}$	$K_{S_D} = e^{9035*\frac{1}{T}-16.35}$	$K_{S_T} = e^{9035*\frac{1}{T}-16.55}$
Pu-2at.%-Ga, 550°C to 625°C	$K_{S_H} = e^{5451*\frac{1}{T}-11.3}$		
Pu-2at.%-Ga, 575°C to 625°C		$K_{S_D} = e^{2970*\frac{1}{T}-8.5}$	
Pu-2at.%-Ga, 350°C to 550°C	$K_{S_H} = e^{6751.04*\frac{1}{T}-12.8}$		$K_{S_T} = e^{6751.04*\frac{1}{T}-13.4}$
Pu-2at.%-Ga, 400°C to 475°C		$K_{S_D} = e^{7070.7*\frac{1}{T}-13.357}$	

** T in Kelvin, some solubilities are estimated (shaded expressions) based on the expected difference in entropy inferred from H and D entropies. A unity pre-exponential constant for dimensioning the expression to units of solubility is assumed (omitted for clarity).*

8. Summary and conclusion.

The utility of Pressure Composition Temperature (PCT) isotherms for Pu and its alloys is made evident in the presented data. The data presented have provided accurate heats and entropies of solution for alloyed and unalloyed Pu. The data have clarified anomalies in the solution behavior of hydrogen in Pu as attributable to spinodal decomposition. The PCT data taken on Pu with low Ga content and Fe impurities indicates stronger spinodal decomposition and therefore greater phase separation. The solubility plots in figure 12 indicate phase depression occurs when hydrogen is present.

Finally, its worth noting that Fukia [10], Flanagan [11] and other researchers [12] have shown that binary alloys, composed of metals A and B, when combined with hydrogen, A-B-H, can result in phase separation of A and B or if hydrogen is already present in one metal, it can also limit or completely prevent mixing of A and B. In a classic example, Fukia demonstrated complete phase separation of a binary alloy in just 250 seconds by a mechanism of hydrogen induced super-abundant vacancy formation with and attendant increase in metal atom self diffusion of 10^5 [10]. So the study of hydrogen in Pu and its alloys may also have great utility in determining the stability of the alloy in addition to understanding corrosion behavior.

Acknowledgements

The authors thank Dr. Matthew Johnson for funding this research and Steve Vigil for his diligence and expertise in operating the Sieverts apparatus.

References

[1] Ward J W, Haschke J M 1994 *Handbook on the Physics and Chemistry of Rare Earths vol 18 (Chapter 123 COMPARISON OF 4f AND 5f ELEMENT HYDRIDE PROPERTIES)* ed K A Gschneider L Eyring G R Choppin and G H Lander (Amsterdam:Elsevier) p327

[2] Mulford R N R, Sturdy G E 1955 *J. Am. Chem. Soc.* 77 3449-3452

Ward J W 1985 *Handbook on the Physics and Chemistry of The Actinides vol. 3 (Properties and Comparitive Trends in Actinide-Hydrogen Systems)* ed A J Freeman and C Keller (North-Holland: Elsevier) p1

Colmenares C, Alexander C 1975 *Lawrence Livermore National laboratory Report UCID-16799 Heat of formation of plutonium hydrides* (Livermore CA USA: Lawrence Livermore Laboratory)

Allen T H 1991 *The solubility of hydrogen in plutonium in the temperature range 475 to 825 degrees centigrade* M.S. Chemistry University of Colorado, Denver

[3] Haschke J M, Allen T H, Morales L A 2000 *Surface and corrosion chemistry of plutonium (Los Alamos Science 26 vol. 1)* pp252-273 (Los Alamos NM USA: Los Alamos National Laboratory)

[4] Wipf H H, 2001 Solubility and diffusion of hydrogen in pure metals and alloys *Physica Scripta* **T94** 43-51

[5] Fukai Y 1993 *The Metal-Hydrogen System: Basic Bulk Properties* (Berlin:Springer)

[6] Mueller W M, Blackledge J P, Libowitz G G 1968 *Metal Hydrides* (New York and London: Academic Press)

[7] Sieverts A 1929 Absorption of Gases by Metals *Zeitschrift f. Metallkunde* **21** 37

[8] Hillert M 1961 A Solid Solution Model for Inhomogeneous Systems *Acta Met.* **9** 526

[9] Cahn J W 1961 On spinodal decomposition *Acta. Met.* **9** 795

Cahn J W 1962 On spinodal decomposition in cubic crystals *Acta Met.* **10** 179

Cahn J W 1962 Coherent fluctuations and nucleation in isotropic solids *Acta Met.* **10** 907

[10] Fukai Y 2003 Formation of superabundant vacancies in M-H alloys and some of its consequences: a review *J. of Alloys and Compounds* **356-357** 263-269

[11] Flanagan T B, Park C 1999 Hydrogen-induced rearrangements in Pd-rich alloys *J. of Alloys and Compounds* **293-295** 161-168

[12] Antonov V, Antonova T, Belash I, Ponyatovskii E 1984 Structure and electrical properties of Pd-Ag-H alloys synthesized at high hydrogen pressures *Phys. Met. Metall.* **57** 671

Hayashi E, Kurokawa Y, Fukai Y 1998 Hydrogen-induced enhancement of interdiffusion in Cu-Ni diffusion couples *Phys. Rev. Lett.* **80** 5588-5590

Tanaka K, Tanaka H, Kawaguchi J 2002 Effects of hydrogenation on interlayer reactions in metallic multilayers *J. of Alloys and Compounds* **330-332** 256